The Influence of Transient Processes on Vapor Intrusion Processes

Y. Yao, K.G. Pennell, E.M. Suuberg*
Brown University, Division of Engineering, 182 Hope Street, Box D, Providence, RI 02912.
Corresponding author phone: (401) 863-1420; e-mail: Eric_Suuberg@Brown.EDU

ABSTRACT

A three dimensional vapor intrusion model was used to investigate the amount of time required to reach steady-state vapor intrusion rates. The effect of pressure fluctuations on vapor intrusion rates was also investigated. These results were obtained for a homogenous soil conceptual site model with groundwater located at 25 feet below ground surface. The time to achieve steady state ranged from approximately 6-12 months depending on geology. However, the time required for crack concentrations to return to zero after a vapor intrusion source had been removed was on the order of years. Pressure fluctuations can result in concentration spikes when the building pressure becomes negative. For highly permeable soils, the instantaneous mass flow rate into the building can be 2 times greater than steady state mass flow rates due to the effect that pressure fluctuations have on soil gas concentration profiles. The results provide insight about managing and characterizing vapor intrusion risks.

INTRODUCTION

Many researchers have cited concerns regarding temporal effects on vapor intrusion phenomenon, but few quantitative analyses have been performed. Tillman and Weaver[1] considered the temporal effects of soil moisture. Mills et al.[2] examined the temporal aspects of vapor intrusion using a 1-D model that included a multicompartmental structure and an exponentially decaying source term. Massmann and Farrier[3] modeled the role of barometric pressure fluctuations on gas transport in the vadose zone and found that barometric fluctuations that occur during storm events can result in atmospheric air penetrating several meters into the vadose zone (in both vertical and horizontal directions).

The present paper investigates transient effects on vapor intrusion using an extension of the three-dimensional (3-D) model, solved using a finite element solver, previously reported by this group[4,5]. The extension in this paper now involves time-dependent terms. The general framework of other 3-D vapor intrusion models incorporates transient equations[6,7,8]; however those model have been primarily employed to predict steady state conditions. The research described herein considers the importance of timescales on pressure fluctuations and the development of soil gas concentration profiles.

MODEL

Table 1 summarizes the equations used in this research. The results presented herein were obtained using the same general modeling approach outlined by Pennell et al.[4] and Bozkurt et al.[5] However, since unsteady conditions were investigated, the governing equations included in this research were time-dependent.

Table 1. General Equations

Soil Gas Flow *Mass Continuity Equation* $\frac{\partial(\eta_g\rho_g)}{\partial t}+\nabla(\rho_g q_g)=0$ *Darcy's Law* $q_g=-\frac{\rho_g k}{\mu_g}\nabla\phi$ where: $\nabla\phi=g\Delta z-\frac{\nabla p}{\rho_g}$ *Transient Flow Equation* $\frac{\partial(\eta_g\rho_g)}{\partial t}=\nabla\left(\frac{k}{\rho_g\mu_g}(\rho_g g\nabla z+\nabla p)\right)$ $(x_p(1-\eta_g)+x_f\eta_g)\frac{\partial p}{\partial t}=\nabla\left(\frac{k}{\mu_g}(\rho_g g\nabla z+\nabla p)\right)$	η_g = Gas filled porosity $\left[\frac{L^3}{L^3}\right]$ ρ_g = Density of gas $\left[\frac{M}{L^3}\right]$ q_g = Velocity of gas $\left[\frac{L}{t}\right]$ k = Intrinsic permeability $\left[\frac{L^3}{L^3}\right]$ μ = Viscosity of gas $\left[\frac{M}{L^3}\right]$ g = Gravity $\left[\frac{L}{t^3}\right]$ z = Vertical position $[L]$ p = Pressure $\left[\frac{M}{Lt^2}\right]$ x_p = Compressibility of solid $\left[\frac{Lt^2}{M}\right]$ x_f = Compressibility of fluid $\left[\frac{Lt^2}{M}\right]$
Chemical Transport equations Mass Continuity Equation $\frac{\partial C_{ig}}{\partial t}+\nabla F_{ig}+R_{ig}=0$ where: $F_{ig}=q_gC_{ig}-D_{ig}\nabla C_{ig}$	D_{ig}= Effective molecular diffusion coefficient for "i" in gas (L^2/t). This was estimated using Millington approach.[9,10] C_{ig} = Concentration of "i" in gas phase Note: the reaction term, R, was not included in the scenarios presented herein.

Figure 1 illustrates the conceptual framework for the model domain. Equilibrium partitioning was assumed to occurr at the 8m deep groundwater contaminant source in a process defined by a Henry's Law constant. Once the contaminants partitioned from the original groundwater source into the soil gas, partitioning from the gas to the soil (sorption) and/or partitioning from the gas phase to the soil moisture was not included. However, it is important to recognize that partitioning of the contaminant might occur between the soil moisture, soil particles and the soil vapor, or between soil vapor and any free phase nonaqueous-phase liquid (NAPL) or nonaqueous-phase solids (NAPS) that might exist in the soil. The role of partitioning within the soil phase is the subject of ongoing research by the authors.

Within the domain of Figure 1, advective soil gas flow is induced by pressure gradients in the soil. The model was exercised for a single building (10 m x 10 m) with a basement (2 m deep) located in the center of an open field (Figure 1). The model was exercised assuming a disturbance pressures (0 Pa or -5 Pa) imposed at the perimeter crack (5mm wide) around the entire floor of the basement. Homogenous geologies were modeled using three different intrinsic soil permeability values ($k = 10^{-10}$, 10^{-11}, and 10^{-12} m^2, plus diffusion only where no disturbance pressure was applied). To ease comparative analysis, a constant effective diffusivity of contaminant (1.04×10^{-6} m^2/sec) was used, regardless of soil permeability. As discussed by Pennell et al.[4] vapor intrusion rates are fairly insensitive to the selection of diffusivity values. The diffusivity value used in this research is a representative of many volatile organic compounds (VOCs).

Figure 1. Schematic of Model Scenario

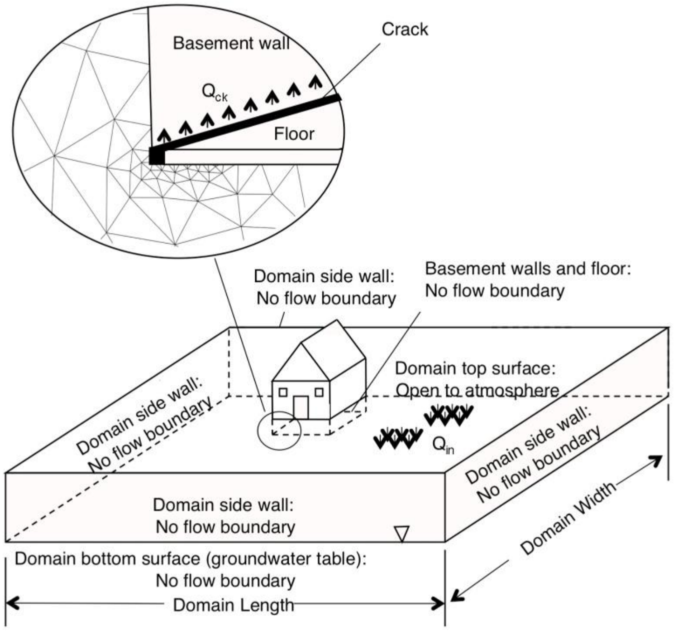

RESULTS

Several different cases were first modeled to investigate the time required to achieve steady state, given changes to the contaminant groundwater sources. Conceptually these conditions were modeled to represent the appearance of a “new” source, and to simulate the effect of groundwater remediation efforts that remove the source. The simulations were conducted assuming a constant indoor disturbance pressure of -5Pa was applied at the crack (except the pure diffusion case where the disturbance pressure was zero).

Transient contaminant source or sink

Figure 2 shows the results for the “new” source case. The concentration at the crack where the disturbance pressure was zero is shown as a function of time assuming that at t=0 the contaminant vapor concentration throughout the domain is zero. The concentration profile develops as a function of time, until the concentration at the crack reaches a steady state value. The highest permeability case ($k=10^{-10}$ m^2) resulted in steady state being reached in the least amount of time (<6 months). This geology is highly permeable and is representing a somewhat rare extreme case. For this case, soil gas concentration profiles are determined by both advective and diffusion transport. For lower, more “typical” permeabilities, soil gas profiles are mainly determined by diffusive flux as can be seen from the lack of permeability dependence in the curves of Figure 2a for $k \geq 10^{-11} m^2$. The time to reach steady state for these soils is nearly twice as long, as compared to the high permeability soil. For $k=10^{-11}$ m^2, advective flux plays a very slight role, but at $k<10^{-12}$ m^2, there is no difference in timescales to reach steady state, regardless of geology; the pure diffusion case lies directly atop the data for $k=10^{-12}$ m^2.

Figure 2. Contaminant concentration at the crack as a function of time. At t=0, the vapor intrusion source appears beneath the whole domain.

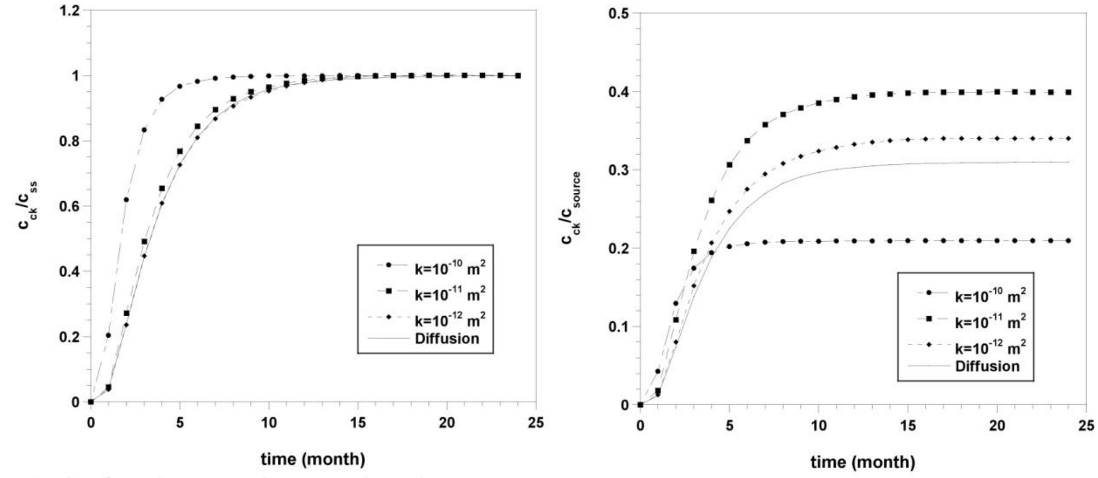

a. Ratio of crack conc. at time, t, and steady state crack conc. vs. time

b. Ratio of crack conc. and source conc. vs. time

Although, steady state occurs over similar timescales for “typical” permeabilities ($k<10^{-10}$ m^2), it is important to note that the steady state crack concentrations are not identical. Figure 2b shows that k=10^{-10} m^2 has the lowest contaminant concentration. This is due to air dilution occurring as a result of advective transport from the surface. The crack concentration for k=10^{-11} m^2 is the highest and is a result of balance between advective transport bringing in dilution air from the groundsurface and advective transport bringing in contaminant mass from the source. As permeability decreases, the concentration at the crack decreases until it reaches a pure diffusive limit, which is approximately 30% of the source concentration.

Figure 3 shows how the soil gas concentration profiles adjust after the vapor intrusion source is removed (instantaneously). At t=0, the source disappears and the soil gas concentrations begin to decrease. The open symbols in Figure 3 represent the situation where the groundwater boundary acts as a sink, i.e. Henry's Law operates to describe dissolution of contaminant in the groundwater. For this case, the soil gas concentrations decrease quickly. However, if the groundwater boundary acts as an impermeable boundary (solid symbols) and does not allow contaminant to leave the domain by dissolving into the water, the crack concentration takes considerably longer to decrease. Again, advective transport plays an important role for k=10^{-10} m^2. For this geology, advective transport results in an increased rate of concentration change. For the other geologies, diffusive transport is dominant, and the corresponding timescales are similar to each other, taking approximately 1 year for the crack concentration to reach 50% of the steady state concentration. It takes approximately 5 years for the crack concentration to approach zero. Figure 3b provides a comparison of crack concentration magnitudes. As previously mentioned, initial steady state crack concentrations are different, but timescales are similar.

Figure 3. Contaminant concentration at the foundation crack as a function of time. At t=0, the vapor intrusion source disappears (instantaneously).

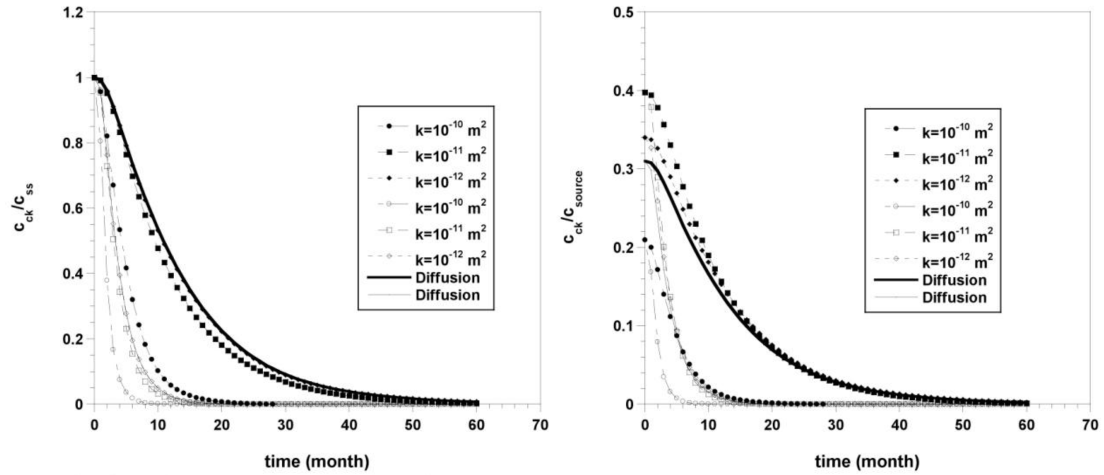

a. Ratio of crack conc. at time, t, and steady state crack conc. vs. time

b. Ratio of crack conc. and source conc. vs. time

The impact of building pressure fluctuations

Simulations were also conducted to investigate the effect of pressure fluctuations. First, the disturbance pressure was cycled between -5 Pa and 0 Pa on a six month cycle (Figure 4a and Figure 4b), which is to simulate the differences in “chimney effect” induced indoor pressure in different seasons. In a second scenario, the disturbance pressure was cycled daily between -5Pa and 0 Pa over a 2 week period (Figure 4c and Figure 4d). For six-month period cycle cases, the switching time for indoor pressure from -5Pa to 0Pa or 0Pa to -5Pa is one day, while a sine function is used to describe transient indoor pressure in one-day cycle cases. For all of these cases, the source concentration was held constant.

Figure 4. Soil gas flow rate with fluctuating disturbance pressures. Figures 4a and 4c illustrate the disturbance pressures that were modeled. The resulting soil gas flow rates are shown in Figures 4b and 4d. Soil gas flow rates are normalized using the steady state value at -5 Pa pressure.

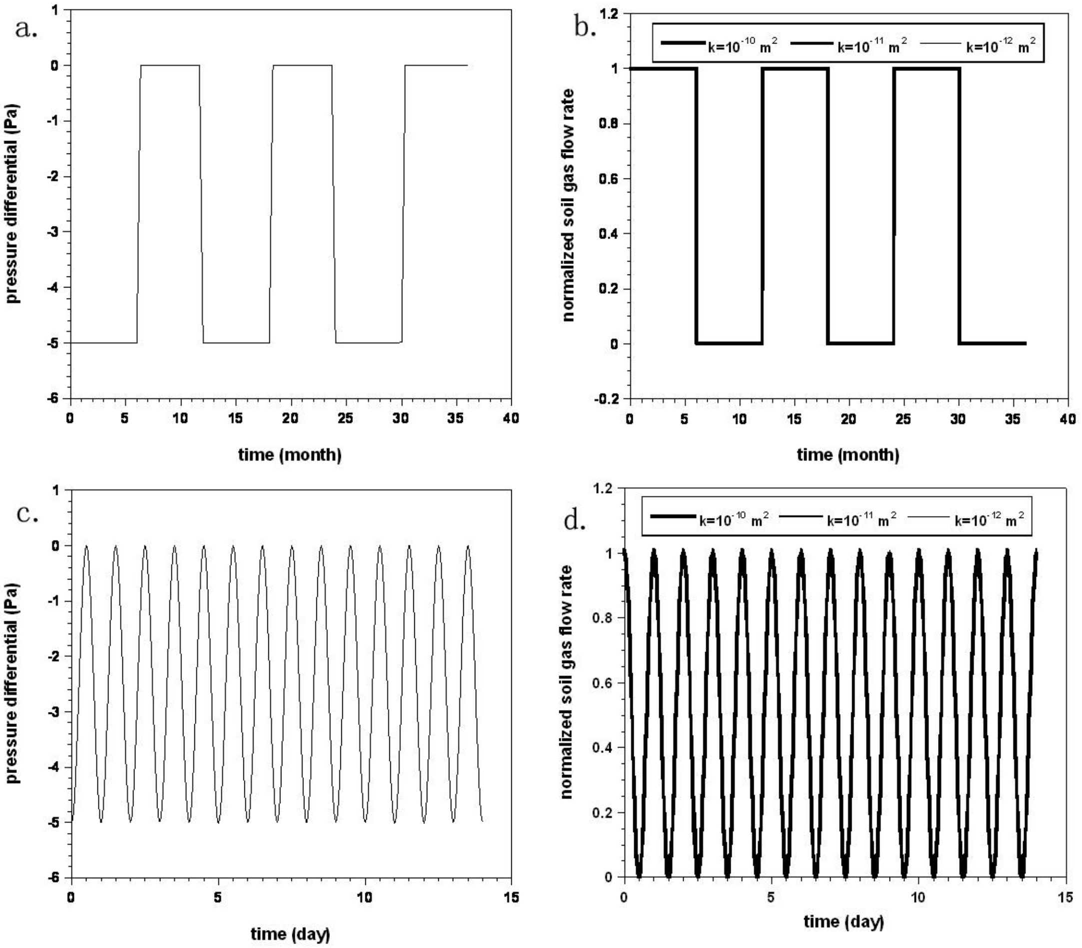

For the six-month pressure cycle (Figure 4a), the soil gas flow rate (Figure 4b) is shown to quickly increase to its maximum value each time the indoor pressure becomes negative. In other words, the pressure profile in the domain responds instantaneously to indoor pressure change, and with it, the advective flow rate. For the short daily indoor pressure cycle (Figures 4c and 4d), a similar phenomenon is observed.

Figure 5 shows the crack concentration as a function of time for the case where pressure was cycled between 0 Pa and -5 Pa with a six-month period. Transient peak contaminant concentrations occur at the crack when the pressure switches from 0Pa to -5Pa. The effect of pressure variation is most significant for the high permeability case ($k=10^{-10}$ m^2). In this case when the indoor pressure becomes zero, the concentration at the crack temporarily sharply drops because of the loss of the ability for advectively drawing in soil gas, but then continues increase to almost twice the -5Pa steady state concentration until the end of the six month period. This is because of the reduced draw of air from the surface. When the disturbance pressure switches to -5Pa, the concentration at the crack quickly jumps to a peak as a result of regaining the ability to convectively draw in soil gas, but then continues to decrease to the steady state -5Pa concentration until the end of that six month period. This repeats every cycle. For the other permeabilities ($k=10^{-11}$ m^2, and $k=10^{-12}$ m^2), convection does not play as significant a role in the mass flow through the crack, and the system quickly reaches steady state after the change of indoor pressure. The lower the soil permeability the less change in concentration is observed upon change in pressure.

To better understand the effect of concentration and soil gas flow rate on contaminant entry into the structure, the more important parameter to consider is mass flow rate through the crack (M_{ck}) (Figure 5c and Figure 5d). Higher Mck values result in higher indoor air concentrations. When the disturbance pressure switches from 0Pa to -5Pa or from -5 Pa to 0Pa, a small peak in M_{ck} is observed for the high permeability case ($k=10^{-10}$ m^2), due to the regain or loss of ability to draw in soil gas.

Figure 5c shows that the contaminant entry rate, relative to the -5 Pa steady state case, is most strongly influenced, in the high soil permeability case ($k=10^{-10}$ m^2). This is understood because of the greater influence of advection in high permeability soils. By the time the permeability decreases to 10^{-12} m^2, there is much less influence of the pressure fluctuation on mass entry rate. Figure 5d also shows that in absolute terms the pressure fluctuation does make a significant difference in mass entry rates into the structure at high soil permeabilities, but not low.

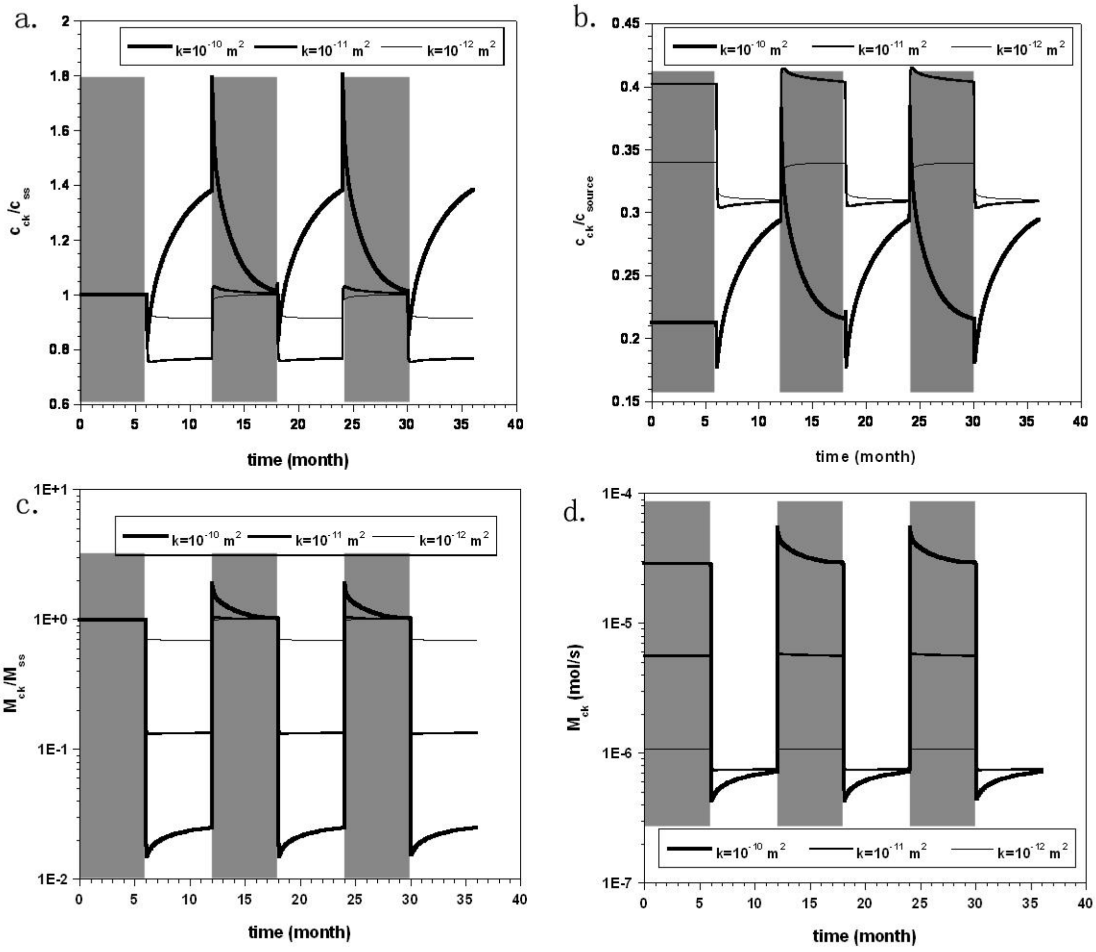

Figure 5. Effect of pressure fluctuations (six month cycle) on crack concentrations and contaminant mass entry rates. C_{ss} and M_{ss} refer to the steady state conditions (-5 Pa) for crack concentration and mass flow rate through the crack, respectively. (Shaded area is at $\Delta p = -5\mathrm{Pa}$)

SUMMARY

The results presented in this paper suggest that the results of vapor intrusion characterization efforts can be significantly affected by vapor transient effects. The mass flow rate of a chemical contaminant entering a house could result in higher indoor air concentrations during certain times of the year, as compared to other times, though the magnitude of the effect greatly decreases with soil permeability. The system reaches steady state quickly, with respect to advective entry.

The results suggest that the timing of indoor air sampling can be important, as indoor air concentration changes simultaneously with the indoor pressure. Cycling of pressures between 0Pa and -5 Pa resulted in contaminant mass flow rates varying by a factor of 2-20, depending how the building is pressurized, and the characteristics of the soils. For low permeability soils , the effects of pressure fluctuations should be modest.

The timescales for adjustment of soil gas concentration to changes in groundwater source concentration are, however, very long. Months or years may be required to see the influence of fluctuations in source concentration on indoor air concentrations.

Additional research is needed to evaluate the effect of chemical partitioning in the soil. Vapor sorption could have a substantial role on vapor migration. The authors are conducting additional research to evaluate those effects.

REFERENCES

1. Tillman, F.D., Weaver, J.W., Temporal Moisture Content Variability Beneath and External to a Building and the Potential Effects on Vapor Intrusion risk Assessment, *Science of the Environment*, **2007**, 379, 1-15.
2. Mills, W.B., Liu, S., Rigby, M.C., Brenner, D., Time-Variable Simulation of Soil Vapor Intrusion into a Building with a Combined crawl Space and Basement, *Env. Sci. Tech.*, **2007**, 41, 4993-5001.
3. Massmann, J. and Farrier, D. F. "Effect of Atmospheric Pressures on Gas Transport in the Vadose Zone." *Water Resources Research*, **1992**, 28(3)777-791.
4. Pennell, K. G., Bozkurt, O., Suuberg, E. M. "Development and Application of a 3-D Finite Element Vapor Intrusion Model" *Journal of the Air and Waste Management Association*, **2009**, 59: 447-460.
5. Bozkurt, O. Pennell, K.G., Suuberg, E.M. "Evaluation of the Vapor Intrusion Process for Non-Homogeneous Soils." *Journal of Ground Water Monitoring & Remediation*, **2009**, 29(1), 92-104.
6. Abreu, L.D., Johnson, P.C. Effect of Vapor source --Building Separation and Building Construction on Soil Vapor Intrusion as Studied with a Three-Dimensional Numerical Model, *Environmental Science and Technology*, **2005**, 39, 4550-4561.
7. Abreu, L.D., Johnson, P.C. "Simulating the Effect of Aerobic Biodegradation on Soil Vapor Intrusion into Buildings: Influence of Degradation Rate, Source Concentrations." *Environmental Science and Technology*, **2006**, 40, 2304-2315.
8. Loureiro, C.O., Abriola, L.M., Martin, J.E., Sextro, R.G., Three-Dimensional Simulation of Radon Transport into Houses with Basements under Constant Negative Pressure, *Environmental Science and Technology*, **1990**, 24, 1338-1348.
9. Millington, R.J., Quirk, J.M., "Permeability of Porous Solids", *Trans. Faraday Soc.*, **1961**, 1200-1207.
10. Millington, R.J., Shearer, R.C., "Diffusion in Aggregated Porous Media", *Soil Sci.*, **1971**, 111, 372-378.

KEYWORDS

Vapor Intrusion, Transient, Pressure Fluctuation